Comparison of the molecular dynamics method and the direct simulation Monte Carlo technique for flows around simple geometries

Eckart Meiburg[a)]
Institute for Theoretical Fluid Mechanics, Bunsenstrasse 10, D-3400 Göttingen, West Germany

(Received 15 May 1985; accepted 3 July 1986)

The molecular dynamics method (MD) and the direct simulation Monte Carlo technique (DSMC) are compared with respect to their capability of simulating vorticity distributions. The statistical assumptions underlying the evaluation of the collision term by the DSMC are analyzed. They lead to the nonconservation of angular momentum for the interaction of particles. Both methods yield equally good results for the Rayleigh–Stokes flow. Using the present parameters, however, only the MD simulation shows the generation of vortices for the flow past an inclined flat plate. This might indicate an effect on the computation of vortical flows. It is suggested that further systematic studies of the effect of the cell size and particle dimensions be carried out.

I. INTRODUCTION

The use of increasingly sophisticated satellites, launch vehicles, and structures in space has been stimulating research on efficient means of transportation among orbits of different altitudes and inclinations (for an overview see Walberg[1]). The payload capacity of such vehicles can be increased significantly by using aerodynamic forces during one or more passes through the atmosphere instead of all-rocket propulsion, leading to the concept of aero-assisted orbit transfer vehicles. As can be seen from Fig. 1, these vehicles will operate under free molecular flow conditions as well as under transitional and continuum flow conditions; the various regimes being characterized by the Knudsen number. Thus there is a need for efficient computational methods for the solution of Boltzmann's equation, which should be able to provide flowfield calculations from small Knudsen numbers through Knudsen numbers larger than unity. According to Bird,[2] for characteristic dimensions such as those that are of interest in flows around space vehicles, the continuum approach breaks down before significant fluctuations set in. This leads us to expect structures in the flowfield even where the Navier–Stokes equations are no longer valid, so we look for computational methods with which we can calculate collisionless flows in the high Knudsen number limit, as well as structures such as vortices in the low Knudsen number limit, together with the related forces and heat transfer rates. The present study investigates the applicability of both the direct simulation Monte Carlo technique described by Bird[2] and the approach first introduced by Alder and Wainwright[3] under the name of molecular dynamics. We want to elucidate the advantages and limitations of these computational methods by simulating flowfields around bodies of simple geometries for various Knudsen and Mach numbers. Our interest focuses on the question of whether or not basic fluid mechanical phenomena such as boundary layers or vortices can be described correctly.

II. MOLECULAR DYNAMICS METHOD VERSUS DIRECT SIMULATION MONTE CARLO TECHNIQUE

Both methods can be used for the simulation of a gas governed by the Boltzmann equation

$$\left(\frac{\partial}{\partial t}+\mathbf{c}\frac{\partial}{\partial \mathbf{r}}+\mathbf{F}\frac{\partial}{\partial \mathbf{c}}\right)f(\mathbf{r},\mathbf{c},t)=\frac{\partial f}{\partial t_{\text{coll}}},$$

which determines the particle distribution function f. Here $\mathbf{r}$ denotes the space vector, $\mathbf{c}$ the velocity vector, and $\mathbf{F}$ an external force acting on the particles. The term on the right-hand side takes the interaction among these particles into account. The simulation methods are based on the fact that this equation can also be formulated for a normalized distribution function, if at the same time the collision cross section of the particles is normalized correspondingly, so that solutions of the Boltzmann equation become independent of the number of particles. For a review see, for example, Derzko.[4]

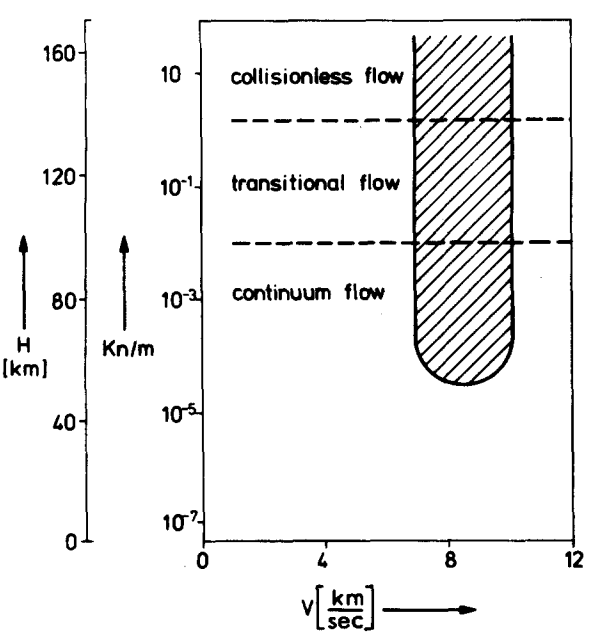

FIG. 1. Flight regimes for aero-assisted orbit transfer vehicles.

[a)] Present address: Department of Chemical Engineering, Stanford University, Stanford, California 94305.

 0031-9171/86/103107-07$01.90

This allows us to employ several thousand particles, all moving with their respective velocities and interacting according to the potential model chosen instead of the much higher number encountered in the real flow. In 1957, Alder and Wainwright[3] first applied their molecular dynamics method, and later, Bird[2] developed a more efficient statistical approach, which became known as the direct simulation Monte Carlo technique (DSMC) and has been applied to a wide variety of free molecular and transitional flows. In the following, a brief description of both methods is given.

A. Molecular dynamics simulation procedure

The calculation starts with the positioning of a given number of particles into the control volume. The initial positions of the particles depend on the physical problem under consideration, which means that they can be randomly distributed or prescribed explicitly. Similarly, the initial velocities are related to the physical problem; they can, for example, have a Maxwell distribution generated with the help of a random number generator. From this point on, the particles move with their individual velocities, subject to certain boundary conditions and to the law of interaction among one another. For an arbitrary particle potential, the calculation proceeds in very small time steps during which the particles move according to their velocities and the forces exerted upon them by the other particles. This force is calculated at the beginning of each time step, so that small steps are required. For the special case of a hard sphere potential, which has been used exclusively in the calculations reported here, particles do not interact except when their paths approach to within one diameter. This allows the time step to be as large as the time span between two subsequent collisions. Therefore, we must first calculate the time of the next collision in the flowfield by examining all particle pairs, then advance all particles up to this time, and finally compute the new velocities of the two particles involved in the collision by means of the laws of classical mechanics. When a particle approaches the boundaries of the control volume, different measures may be taken, varying according to the physical problem. The particle can be specularly reflected, which corresponds to a symmetry boundary condition, or it can be diffusely reflected, thus simulating a rigid wall. In this case, a new velocity would be calculated for the particle from the temperature of the wall. We can also apply an accommodation coefficient, which takes into account the extent to which the post-collision particle velocity depends on its pre-collision history. A periodic boundary condition can be simulated by placing the particle back into the flowfield close to the opposite boundary. Macroscopic quantities can be calculated at arbitrary times by sampling the properties of the particles.

As Alder and Wainwright already mentioned in their original paper, improving the computational procedure of selecting the collision partners and carrying out the collisions leads to a considerable speed-up of the calculation. Modern vector computers such as the CRAY-1S, on which all calculations reported here were performed, offer new opportunities in this regard (for details see Meiburg[5,6]). The molecular dynamics simulation procedure has the advantage of being a grid-free method. This allows the treatment of relatively complicated configurations, since in principle the only requirement to be satisfied by the geometry of the control volume or of a body in the flow is that it must allow us to calculate the time at which a particle will cross a boundary when its position and velocity are known. Thus it is easily feasible to calculate, for example, flows around satellites, as long as their shapes can be composed of cylinders, cones, planes, and other basic geometries.

B. Direct simulation Monte Carlo technique (DSMC)

This technique is similar to the molecular dynamics method in that it computes the trajectories of a large number of particles and calculates macroscopic quantities by sampling particle properties, but it has the advantage of being more efficient on electronic computers. It has been successfully applied to the simulation of a large variety of rarefied gas flows. A detailed description is given in Bird.[2] The DSMC differs from the molecular dynamics approach in the way interactions among the particles are treated. The place and time of a collision are no longer determined by comparing the trajectories of all particles, but by means of a statistical consideration. The principle steps of the DSMC are as follows: At the beginning of the calculation, the flowfield is divided into a net of cells. The particles are positioned into the cells in the same way as in the molecular dynamics method. The computation now proceeds in small discrete time steps Δt over which the motion of the particles and their interactions are uncoupled. Within one time step, all particles are first advanced according to their individual velocities, with the boundaries taken into account as in the molecular dynamics method. Then in each cell a certain number of statistical collisions is computed in the following way: From all the particles in the cell, two are selected randomly, without consideration of their actual positions. Then a "collision" between these two particles is computed as described below. It was shown by Bird[2] that this collision corresponds to a time increment

$$\Delta t_{\text{coll}} = 2/N\pi d^2 n c_{\text{rel}},$$

for hard sphere particles that have been used exclusively here. In this equation, N is the number of particles in the cell, πd^2 is the collision cross section of the particles, n represents the number density, and c_{rel} denotes the relative velocity of the particles involved in the collision. Further collisions are carried out until the sum of the time increments Δt_{coll} has reached the size of the time step Δt for each of the cells. For a sufficiently large number of particles per cell, this procedure yields the correct collision rate. The time step Δt should be small compared to the mean collision time, and the cell dimensions should be small compared to the mean free path, in order to yield accurate results.

A problem that arises from the calculation of "statistical collisions" will be discussed in the following. In general, the six post-collision velocity components u_1', v_1', w_1' and u_2', v_2', w_2' of two particles of mass m and pre-collision velocity components u_1, v_1, w_1 and u_2, v_2, w_2 undergoing an elastic collision are completely determined by:

(a) conservation of linear momentum per mass

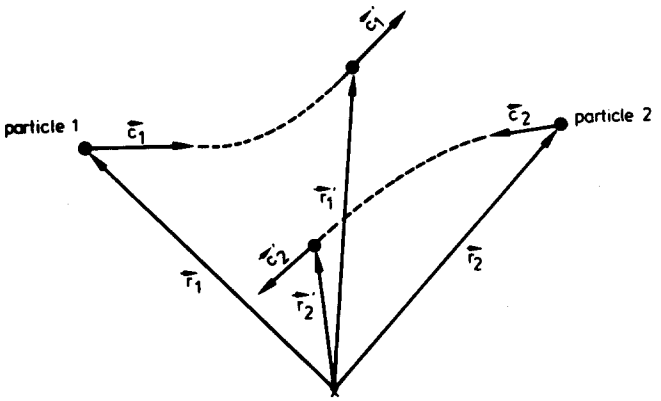

FIG. 2. Particle position and velocity vectors for a binary collision.

$$u_1' + u_2' = u_1 + u_2, \quad v_1' + v_2' = v_1 + v_2,$$
$$w_1' + w_2' = w_1 + w_2,$$

(b) conservation of kinetic energy per mass

$$u_1'^2 + v_1'^2 + w_1'^2 + u_2'^2 + v_2'^2 + w_2'^2 = u_1^2 + v_1^2 + w_1^2 + u_2^2 + v_2^2 + w_2^2,$$

(c) conservation of angular momentum per mass

$$\mathbf{r}_1' \times \mathbf{c}_1' + \mathbf{r}_2' \times \mathbf{c}_2' = \mathbf{r}_1 \times \mathbf{c}_1 + \mathbf{r}_2 \times \mathbf{c}_2,$$

(d) particle potential ϕ

$$\frac{\ddot{\mathbf{r}}_1}{m} = -\frac{\ddot{\mathbf{r}}_2}{m} = -\frac{d\phi}{ds},$$

where $\mathbf{r}_1, \mathbf{r}_2, \mathbf{r}_1', \mathbf{r}_2'$ are the pre- and post-collision particle position vectors (Fig. 2) and s is the distance between the particles. Since in the DSMC we try to calculate a collision between particles without considering their positions, the particle potential cannot be used to compute the post-collision velocities directly. But it can be shown that in a statistical sense, for the hard sphere particle potential, all directions are equally probable for the post-collision relative velocity of the two particles. This leads to the following method of computing collisions in the DSMC. First, the direction of the post-collision relative velocity is determined by randomly selecting an azimuthal and a polar angle. Then the four degrees of freedom remaining are used to satisfy the conservation of linear momentum and energy. Now the conservation of angular momentum can no longer be satisfied. Thus the DSMC yields both post-collision velocities sketched in Fig. 3

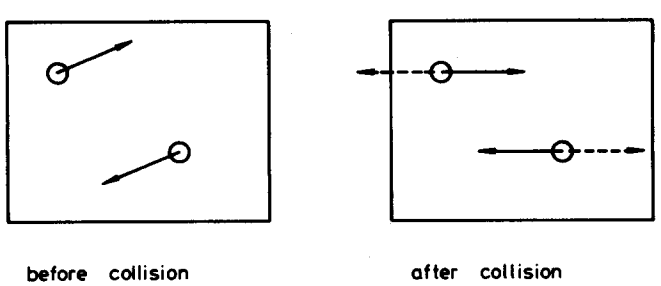

FIG. 3. Pre- and possible post-collisional velocities of two particles in a cell. The DSMC does not conserve angular momentum, since both the solid and the dashed velocity vectors present equally possible post-collisional particle velocities.

with equal probability. This is obviously incorrect, leading us to suspect that the DSMC might not correctly describe flowfields in which angular velocities are of importance, such as vortical flows. The nonconservation of angular momentum results from the fact that we are trying to calculate an interaction between two particles without considering their actual position. As long as this principle is employed, the effect of violating the law of conservation for angular momentum will therefore be seen, even for other particle potentials than the hard sphere. Obviously, the error depends on the distance between the interacting particles, and since these are always selected from the same cell, the error is expected to depend on the cell size. In principle, however, it will remain present even for small cells.

III. RESULTS

A. Impulsively started flat plate

As a test example for the two simulation methods described above we selected the flow induced by an infinite flat plate impulsively started from rest in its own plane in a compressible fluid, which had previously been considered by Bird.[2] Van Dyke[7] treated this problem by means of matched asymptotic expansions. Becker[8] generalized the boundary layer solution with respect to suction and blowing as well as to a change in the temperature of the plate. If ρ_0 is the density at the wall and y is the distance from the wall we can define the coordinate transformation

$$y' = \int_0^y \frac{\rho}{\rho_0}\, dy.$$

For u_w denoting the wall velocity, t the time, and ν_0 indicating the viscosity at the wall we obtain, for large Reynolds numbers, the similarity solution for the dimensionless velocity having the form

$$u/u_w = \operatorname{erfc} \eta,$$

where

$$\eta = y'/2\sqrt{\nu_0 t}\ .$$

Figure 4 compares the numerical results from both a MD calculation and a DSMC simulation each employing

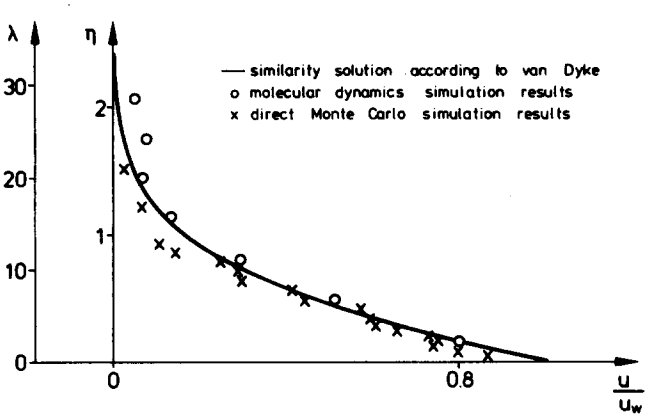

FIG. 4. Molecular dynamics and direct Monte Carlo simulation results compared to the exact solution for the impulsively started flat plate, Re = 85. Here η denotes the similarity variable and λ indicates the distance from the wall in mean free paths.

20 000 particles with the exact solution. We find that, apart from statistical scatter, the values agree quite well, provided that the dimension perpendicular to the plate of the cells in the DSMC simulation is small enough. As long as that is the case, then the fact that angular momentum is not conserved does not have a strong impact on the results. This can be explained by an analysis of the rate at which u-momentum is transferred from the wall to the flow. If the cell size is large compared to the mean free path of the flow, a particle that has just been reflected from the wall can be selected to collide with another particle in the same cell but relatively far away, and with a u-velocity considerably smaller than the velocity of the wall. Since angular momentum is not conserved, both particles will, on the average, have the same u-velocity after the collision. This results in an unrealistic deceleration of the particle close to the wall. As this particle is likely to hit the wall much earlier than the one farther away, the rate of transfer of u-momentum to the flow will be too high. If, on the other hand, the cell size close to the wall is small compared to the mean free path, a particle that has just been reflected from the wall will undergo the next collision four or five cells away from the wall. This in turn means that it is approximately the same distance from the wall as its collision partner, so that, on the average, both collision partners will hit the wall at the same time. Thus it is unimportant which one of them has the higher, and which one the lower u-velocity after the collision, so that in this case the conservation of angular momentum is without significance for the rate of transfer of u-momentum. With the rate of transfer of momentum being computed accurately, the DSMC can be expected to yield accurate results for the flowfield described above.

B. Vortex shedding behind an inclined flat plate

The process of vortex shedding is a classical problem in fluid mechanics. Experimentalists as well as theoreticians have carried out numerous investigations to shed light on different aspects of the problem, such as the generation and separation of vortices, the stability of vortex streets, the transition to turbulent wakes, the forces involved, or the possibilities of manipulating or suppressing the shedding process. For reviews of this topic, see for example, McCroskey,[9] Bearman and Graham,[10] and Bearman.[11] Most studies have been concerned with the incompressible flow around bodies of simple geometries, such as circular cylinders, thin flat plates, rectangular prisms, or cones. For example, Goldburg, Florsheim, and Washburn[12] have shown that vortex shedding also occurs in hypersonic flows, so the phenomenon seems to bear some relevance for the flow around space vehicles in the upper atmosphere. It is unknown, however, at which Knudsen numbers we can expect vortex street wakes. This gives rise to the question as to whether computational techniques for the solution of the Boltzmann equation—upon which a calculation of such flowfields must be based—are able to describe the generation and behavior of vortices. This in turn is a prerequisite for obtaining correct values for the related forces such as those acting upon the flaps with which the Space Shuttle is maneuvered.

As a model problem we studied the flow around a flat plate at 45° incidence, by means of an MD simulation as well as a DSMC simulation. The length of the plate d was 60 mean free paths, resulting in a Knudsen number of 0.017. The Mach number was 0.7, and the Reynolds number based on the length of the plate was 78. Both experiments and theoretical considerations suggest that the flow is unstable at this Reynolds number. The Knudsen number corresponds to the flow around a flat plate of 0.4 m at an altitude of 100 km. In order to avoid difficulties with the downstream boundary condition, the plate was impulsively started from rest and then towed through the three-dimensional control volume at constant speed, as shown in Fig. 5. Symmetry conditions were applied at all boundaries, so that no boundary layers form and the blockage effect is less severe than for a solid wall. Experiments have shown that blockage effects influence the onset of vortex shedding in incompressible low Re-number flows (Shair *et al.*[13]), but it is unknown so far how important blockage effects are in compressible low Re-number rarefied flows. When a particle collided with the plate, it was given a new velocity according to a Maxwellian distribution formed with the temperature of the plate. This corresponds to diffuse reflection of the particles at the plate, i.e., the accomodation coefficient was taken as 1.

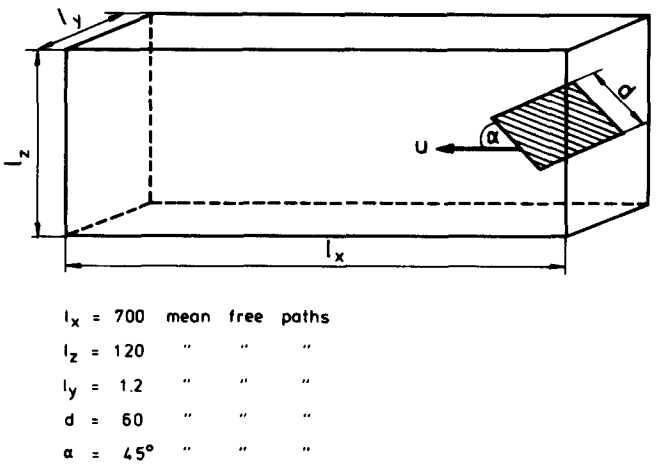

FIG. 5. Control volume for the simulation of vortex shedding behind an incline flat plate.

The MD calculation was carried out in a fully three-dimensional way. Because of CPU time and storage constraints, the number of particles had to be limited to 40 000 for this simulation, resulting in the relatively large molecular diameter of 0.753 mean free paths. This means that a fraction of approximately 8.9% of the control volume was occupied by the particles. In contrast to the MD simulation, which for the calculation of realistic collisions has to consider the positions of the particles in both x, y, and z direction, the DSMC simulation can be carried out in two dimensions as a consequence of the fact that it deals with a statistical set of collisions. The higher computational efficiency of the DSMC allowed us to employ 210 000 particles for the simulation of the flow past the inclined flat plate. The hard sphere potential was applied in both cases. The results had to be smoothed in order to be able to illustrate the flowfield by means of instantaneous streamlines and lines of constant

vorticity as well as plots of velocity vectors. These continuum–mechanical data were obtained by averaging the properties of particles in a net of cells, with the depth of the cells for the MD simulation being equal to the depth of the control volume. This means that, although the simulation was carried out in three dimensions, the results discussed in the following were obtained by integrating over the spanwise direction. In order to give an impression of the direction of the flow everywhere in the field, we integrated piecewise streamlines from a given grid of starting points. Their strong curvature in some regions indicates the presence of vortices, whereas their length does not have any physical meaning. The magnitude of the velocity is proportional to the length of the velocity vectors. Lengths have been nondimensionalized by the mean free path, and time has been made dimensionless with the length and the velocity of the plate.

First we will discuss the results of the MD simulation. Soon after the start of the plate, at time 0.36, the streamlines in the reference frame moving with the plate clearly follow the geometry of the plate (Fig. 6). Although the flow seems to have separated at the top, a vortex is not yet visible. Due to the inevitable statistical scatter, the exact position of the separation point cannot yet be recognized. The scatter is responsible for some streamlines' ending on or leaving from the plate. The separating streamline at the rear tip has not yet become tangential to the plate. The velocity vectors show a strong deceleration of the flow immediately behind the plate. At time 1.07, we can recognize for the first time a region of recirculating flow on the upper side of the plate (Fig. 7). The front stagnation point is close to the tip, and separation occurs immediately behind the upper tip. The vorticity distribution now shows a maximum close to the center of the vortex. The separating streamline at the lower tip is now almost tangential to the plate. A little later at time 2.31, we notice that the vortex has increased in strength with its cen-

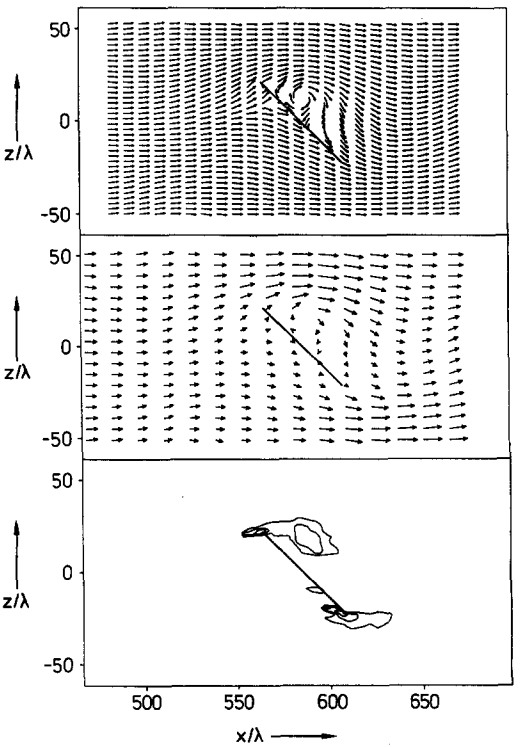

FIG. 7. Molecular dynamics simulation: streamlines, velocity vectors, and contours of constant vorticity at time 1.07.

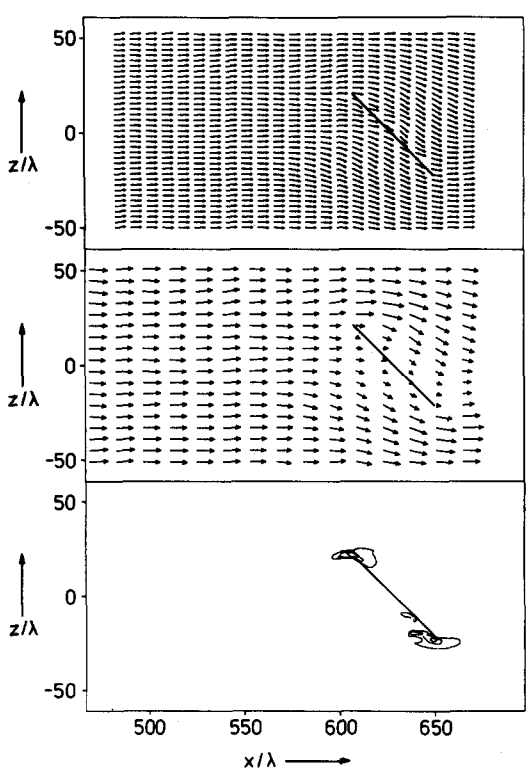

FIG. 6. Molecular dynamics simulation: streamlines, velocity vectors, and contours of constant vorticity at time 0.36.

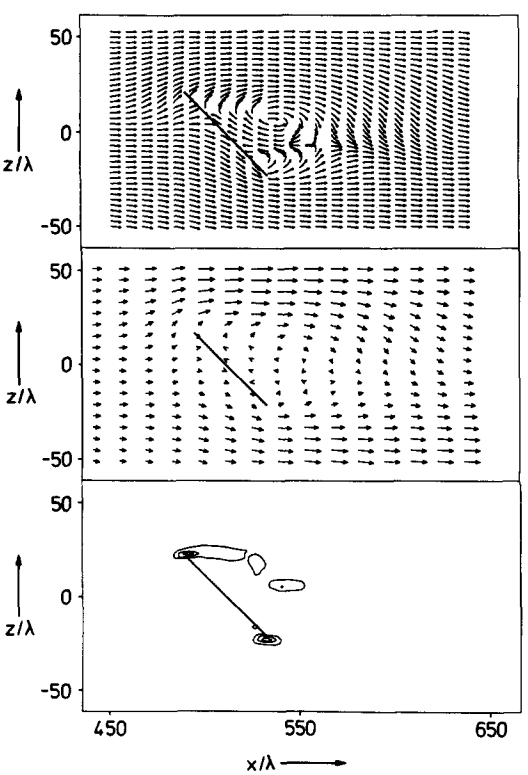

FIG. 8. Molecular dynamics simulation: streamlines, velocity vectors, and contours of constant vorticity at time 2.31.

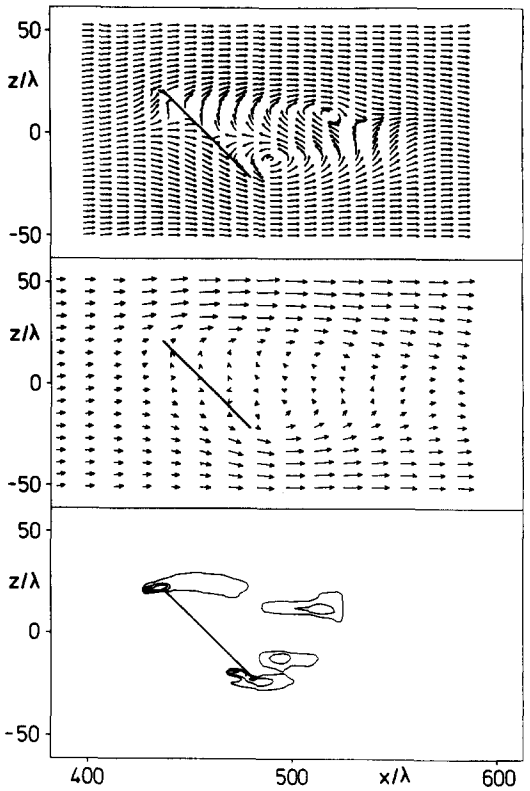

FIG. 9. Molecular dynamics simulation: streamlines, velocity vectors, and contours of constant vorticity at time 3.19.

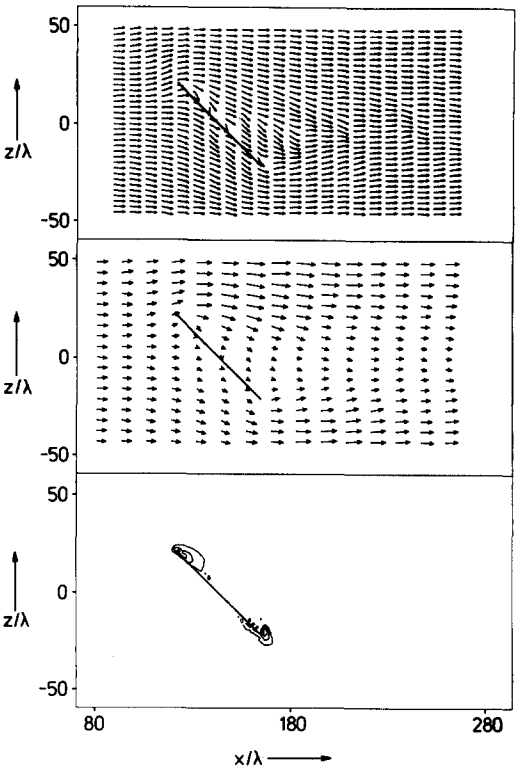

FIG. 10. Direct Monte Carlo simulation: streamlines, velocity vectors, and contours of constant vorticity at time 8.44.

ter having moved downstream, thus causing a second region of recirculating flow to form close to the lower tip (Fig. 8). At time 3.19, the region has grown to a full vortex, while at the same time the center of the initial vortex has moved further downstream. The maxima of the vorticity distribution again correspond to the centers of the vortices (Fig. 9). From this point on, periodic vortex shedding can be observed with alternating left-and right-rotating vortices forming behind the tips of the plate and moving downstream. The Strouhal number formed with the projection of the plate perpendicular to the oncoming flow is 0.25. For a Reynolds number as low as 78, this seems to be too high when compared with experimental results for incompressible flows. One reason for this discrepancy probably lies in the fact that the channel is fairly narrow, thus causing a strong acceleration of the flow above and below the plate, which in turn leads to separation of the vortices before they reach their full size.

The corresponding two-dimensional DSMC simulation yielded quite different results. The number of particles per cell was taken as 20 and the size of the cells came to approximately 2.9 mean free paths, which is small compared to the scale of the macroscopic vortices expected to be generated, but larger than the mean free path. Here too, at time 8.44 the flow follows the shape of the plate, and the maximum of the velocity production lies close to the tips of the plate (Fig. 10). However, it "diffuses" very quickly, so that no macroscopic vortices can form. The reason for this is believed to lie partly in the nonconservation of angular momentum. The vorticity that is continuously being generated at the surface of the plate as a consequence of the no-slip condition, i.e., diffuse reflection, decays in the process of the calculation of collisions. This means that close to the wall, there is still enough vorticity to cause local separation and recirculation of the flow, but the formation and separation of large scale vortices does not occur.

The difference between the MD and the DSMC results is further reflected in the streamline pattern of the whole flowfield at the end of each calculation. The pattern obtained from the MD calculation (Fig. 11) clearly shows the waviness of the wake indicating the presence of vortices moving downstream from the plate. The corresponding pattern of

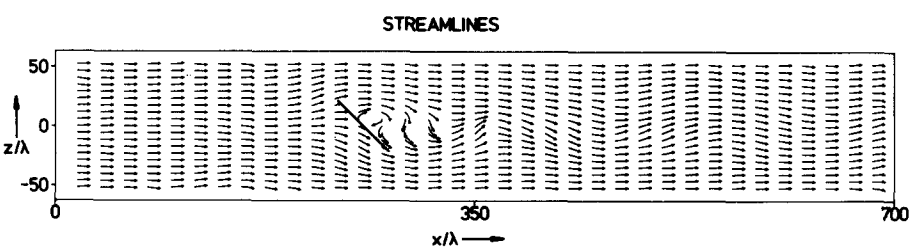

FIG. 11. Molecular dynamics simulation: streamline pattern at time 6.55.

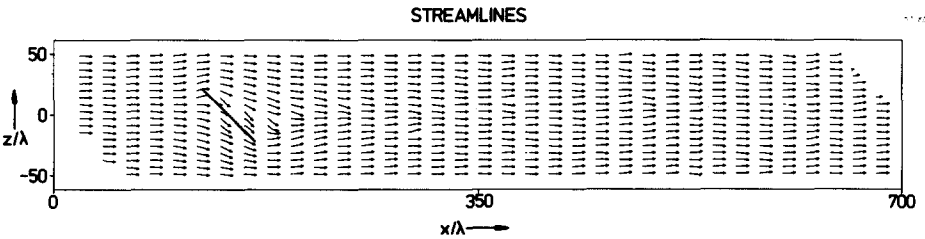

FIG. 12. Direct Monte Carlo simulation: streamline pattern at time 8.44.

the DSMC simulation (Fig. 12), on the other hand, does not show this waviness.

The degree to which angular momentum and vorticity are being "diffused" in the process of carrying out the collisions obviously can depend on the cell size as well as on the number and size of the particles used. The early destruction of angular momentum in the regions of high shear behind the tips of the plate might be reduced by using a locally refined mesh. The relatively large particle diameter in the MD simulation, on the other hand, results in the molecules' occupying a considerable fraction of the control volume, which could cause some dense gas effects and thus influence the diffusion of vorticity at the scale of the particle size. Therefore, a systematic study of the effect of the cell size in the DSMC on the nonconservation of angular momentum and vorticity should be carried out, and the influence of the number and size of particles on both the DSMC and the MD results presented here should be checked. It would be convenient to define a simpler test problem for this purpose, since on presently available computers it would be too costly to reduce the cell size used in the DSMC by a factor of, say, 10 and keep the number of particles per cell constant. This systematic study might help to clarify to what degree the loss of angular momentum depends on the numerical parameters such as the cell size and the number of particles. Even if the loss of angular momentum can be reduced by a large amount by using much smaller cells, the fact that a certain number of particles per cell has to be maintained could considerably reduce the numerical efficiency of the DSMC as compared to the MD for some transitional flows. This is of interest for future applications, which will certainly include calculations of flowfields around bodies in regimes where the mean free path is small compared to the dimensions of the body.

IV. CONCLUSIONS

Within the present study, two numerical methods for the simulation of Boltzmann's equation—the molecular dynamics method and the direct simulation Monte Carlo technique—have been compared with respect to their capability of calculating flows with strong gradients in the vorticity distribution. The goal was to study the effect of the statistical assumptions underlying the evaluation of the collision term in the Boltzmann equation by the DSMC technique, which lead to the nonconservation of angular momentum for the interaction of particles. Both methods yielded satisfactory results for the Rayleigh–Stokes problem. For the numerical parameters investigated here, however, the DSMC calculation for the flow past an inclined flat plate did not show periodic vortex shedding, whereas the MD simulation resulted in a vortex street, as was demonstrated by means of streamline-, vorticity-, and velocity-vector plots. The difference in the results is believed to be related to the loss of angular momentum on the particle level during the process of carrying out the collisions. Further work on a simpler test problem should be carried out in order to systematically investigate the effect of the cell size as well as the number and size of the particles on the loss of angular momentum and vorticity. Such a study would not only help to answer the question whether or not the DSMC in its present version has principle problems in simulating vortical flows, but would also allow conclusions with regard to the computational efficiency of both methods, which might favor the MD for some transitional flow problems if the DSMC requires cells that are too small. For large Knudsen number flows, however, there seems to be no doubt that, due to its higher numerical efficiency, the DSMC is to be preferred.

A possible next step may be the development of a hybrid scheme that is based on the MD approach where vortices are expected, and that works with the DSMC everywhere else. This would allow a combination of the advantages of both methods.

ACKNOWLEDGMENTS

I would like to express my thanks to Professor H. Oertel, who supervised this work, for his personal involvement and valuable advice that he provided during many helpful discussions, and to Dr. R. Kessler for giving a preliminary review of the manuscript.

[1]G. D. Walberg, AIAA Paper 82-1378, 1982.
[2]G. A. Bird, *Molecular Gas Dynamics* (Clarendon, Oxford, 1976).
[3]B. J. Alder and T. Wainwright, in *Proceedings of the International Symposium on Transport Processes in Statistical Mechanics* (Interscience, New York, 1957), p. 97.
[4]N. A. Derzko, UTIAS Rev. **35**, 1 (1972).
[5]E. Meiburg, in *Vectorization of Computer Programs with Application to Computational Fluid Dynamics* (Vieweg, Wiesbaden, 1984), p. 235.
[6]E. Meiburg, DFVLR Forschungsbericht **85**, 13 (1985).
[7]M. van Dyke, Z. Angew. Math. Phys. **3**, 343 (1952).
[8]E. Becker, Z. Angew. Math. Phys. **11**, 146 (1960).
[9]W. J. McCroskey, J. Fluid Eng. **99**, 8 (1977).
[10]P. W. Bearman and J. M. R. Graham, J. Fluid Mech. **99**, 225 (1980).
[11]P. W. Bearman, Annu. Rev. Fluid Mech. **16**, 195 (1984).
[12]A. Goldburg, B. H. Florsheim, and W. K. Washburn, AIAA J. **3**, 1332 (1965).
[13]F. H. Shair, A. S. Grove, E. E. Petersen, and A. Acrivos, J. Fluid Mech. **17**, 546 (1963).